Wideband Deterministic All-Order Polarization-Mode Dispersion Generation via Pulse Shaping

Houxun Miao, *Student Member, IEEE*, Andrew M. Weiner, *Fellow, IEEE*, Leo Mirkin, and Peter J. Miller

***Abstract*—We developed a wideband deterministic all-order polarization-mode dispersion (PMD) generator which is based on ultrafast pulse shaping techniques. We demonstrated generation of arbitrary desired PMD profiles with variable mean differential group delays ranging from 2 to 5 ps over ∼10-nm bandwidth.**

***Index Terms*—Optical fiber communications, polarization-mode dispersion (PMD), ultrafast pulse shaping.**

I. Introduction

POLARIZATION-MODE dispersion (PMD) remains a challenge in high-speed optical fiber telecommunication systems [1]. PMD arises from the random birefringences in optical fibers due to the imperfect symmetry in the fiber core. PMD is described by the 3×1 PMD vector $\vec{\tau}(\omega)$, where the magnitude defines the differential group delay (DGD) and the direction is aligned with the slow principal state of polarization (PSP). To characterize all-order PMD-induced system outages in the laboratory, it is essential to have a PMD generator that can quickly generate arbitrary frequency-dependent PMD profiles in the all-order regime expected in optical fiber links. Most current PMD emulators are constructed by using several birefringent segments with either fixed or variable DGDs [2]. The stochastic feature of PMD is generated by adjusting the orientation of these segments. The drawbacks are: 1) a large amount of birefringent segments is necessary to emulate the frequency-dependent and time-stochastic features of the PMD in real fiber links; 2) it is extremely difficult to generate an arbitrary PMD profile in the all-order regime. In previous work [3], we demonstrated generation of arbitrary frequency-dependent DGD profiles by applying ultrafast pulse shaping (or equivalently, wavelength-parallel processing) techniques [4]. Due to the limitation of the two-layer liquid crystal modulator array (LCM) incorporated in the pulse shaper, the DGD generator cannot generate arbitrary desired frequency-dependent DGD and PSP profiles simultaneously. In this letter, we treat all-order PMD effects as a frequency-dependent Jones matrix. By using a transmission pulse shaper incorporating a four-layer LCM, we can generate any desired frequency-dependent Jones matrix over a bandwidth of ∼10 nm with a spectral resolution approaching 11.6 GHz. Thus, we can deterministically and repeatably generate specific all-order PMD instances.

Manuscript received September 17, 2007; revised October 18, 2007. This work was supported in part by the National Science Foundation under Grant 0501366-ECS.

H. Miao and A. M. Weiner are with the School of Electrical and Computer Engineering, Purdue University, West Lafayette, IN 47907-1285 USA (e-mail: hmiao@purdue.edu; amw@ecn.purdue.edu).

L. Mirkin and P. J. Miller are with CRI Inc., Woburn, MA 01801 USA (e-mail: LMirkin@cri-inc.com; PJMiller@cri-inc.com).

Color versions of one or more of the figures in this letter are available online at http://ieeexplore.ieee.org.

Digital Object Identifier 10.1109/LPT.2007.912494

II. Theory

In the absence of polarization-dependent loss/gain, the frequency-dependent Jones matrix of a fiber link (isotropic chromatic dispersion excluded) is given in the Caley/Klein form [5] $U = \begin{bmatrix} \cos\theta e^{j\phi} & \sin\theta e^{j\psi} \\ -\sin\theta e^{-j\psi} & \cos\theta e^{-j\phi} \end{bmatrix}$, where θ, φ, and ψ are frequency-dependent angles. The Jones matrix can be written as the multiplication of three elementary rotation matrices

$$U = \begin{bmatrix} \exp(j\theta_1) & 0 \\ 0 & \exp(-j\theta_1) \end{bmatrix} \begin{bmatrix} \cos\theta_2 & j\sin\theta_2 \\ j\sin\theta_2 & \cos\theta_2 \end{bmatrix} \times \begin{bmatrix} \exp(j\theta_3) & 0 \\ 0 & \exp(-j\theta_3) \end{bmatrix} \quad (1)$$

where $\theta_1 = (\varphi + \psi)/2 + \pi/4$, $\theta_2 = -\theta$, and $\theta_3 = (\varphi - \psi)/2 - \pi/4$. To realize wavelength-parallel Jones matrix generation, we apply ultrafast pulse-shaping techniques to realize the frequency-dependent Jones matrix as a space-dependent Jones matrix at the focal plane of the pulse shaper, where a four-layer LCM array generates the three elementary rotation matrices independently at each spatial pixel. Each LCM layer functions as a linear retarder array (128 pixels) with specified fast/slow axes and arbitrarily adjustable retardance. The orientations of the slow axes of the four LCM layers are 90°, 0°, 45°, and 0°, respectively. We operate the last three layers (0°–45°–0°) to produce the three elementary rotation matrices on the right side of (1). After the operation for Jones matrix generation, an isotropic spectral phase of $\theta_1 + \theta_2 + \theta_3$ remains. To correct this residual phase, we apply an additional phase to the first and second LCM layers and program them in common-mode, which results in a polarization-insensitive phase-only modulation functionality. Note, the second LCM layer is programmed for the superposition of the phase for Jones matrix generation and the common-mode residual phase correction.

III. Experimental Setup and Results

Fig. 1 shows our experimental setup for PMD generation and measurement (to check the performance of PMD generation). A transmission pulse shaper incorporating a four-layer LCM functions as the PMD generator. The pulse shaper works in this way: the first grating-lens pair spreads different frequency components of the input signal spatially at the focal plane, then special light modulation is applied via the LCM, after that, different frequency components of the signal are recombined through another lens-grating pair. Each of the 128 LCM pixels

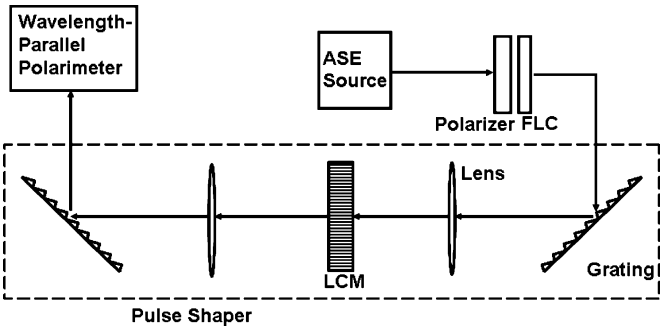

Fig. 1. Experimental setup.

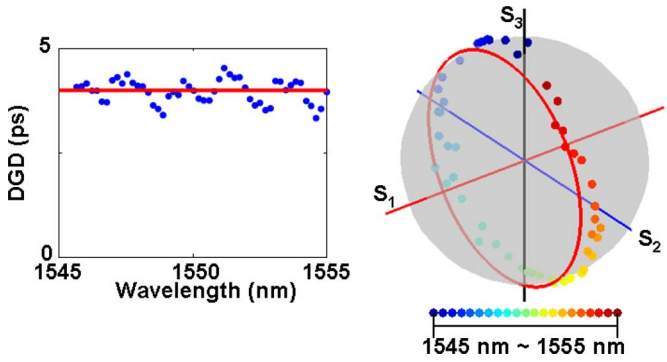

(a) (b)

Fig. 2. (a) Measured (dots) and target DGD profiles (solid lines). (b) Measured (dots) and target PSP profiles (solid line) on the Poincare sphere.

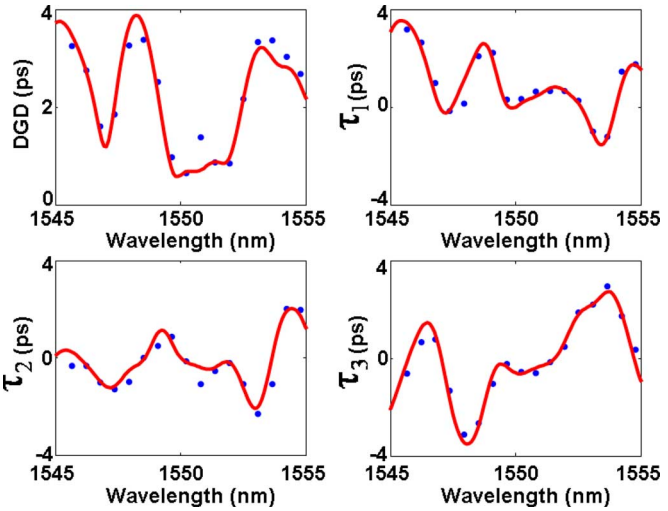

Fig. 3. Measured (dots) and target (solid lines) profiles of DGD and three PMD components for 2-ps mean DGD.

can be programmed independently to obtain different Jones matrices, as required to realize the desired frequency-dependent Jones matrix profile. The updating time of each LCM layer is ∼100 ms (limited by the control electronics), which limits the updating time of the PMD generator to ∼500 ms. An amplified spontaneous emission (ASE) source followed by a polarizer is used to produce a wideband optical signal with 0° linear state of polarization (SOP) for PMD measurement. A ferroelectric liquid crystal (FLC) retarder is used to switch the input SOP between 0° linear and right-hand circular (RHC) states. The signal is then launched into the PMD generator. The output SOPs are measured with a home-developed wavelength-parallel polarimeter [6]. The polarimeter consists of a collimator, a pair of FLC retarders, a polarizer, a grating, a lens, and a linear InGaAs detector array The spectral resolution of the polarimeter is 23.8 GHz. The generated PMD profiles are calculated with the measured output SOPs by applying the Müller matrix method (MMM) [7].

In a first experiment, we generate the PMD profile of a concatenation of two PM fibers, where the DGD is a constant and the frequency-dependent PSPs form a circle on the Poincare sphere. We first use a computer to simulate the PMD profile and the frequency-dependent Jones matrix of the concatenation of two PM fibers with DGDs of 3.91 and 0.79 ps. The slow axes of the two PM fibers are 45° and 0°. We then program the pulse shaper according to the predicted Jones matrix and measure the generated PMD profile by MMM. Fig. 2 shows the measured DGD and PSP profiles together with the target ones for comparison. The estimated root-mean-square (rms) error of the generated DGD is 0.285 ps, 7.1% the target DGD; and the PSPs fall close to the target PSP circle. This indicates good performance of the PMD generation and measurement.

For all-order PMD generation, we first simulate and store via computer the PMD profiles and frequency-dependent Jones matrix of a single-mode fiber by using the Foschini–Poole model [8], where a large amount of random oriented birefringent sections (small birefringence) are used. Then the stored Jones matrix is applied via the pulse shaper and the generated PMD profiles are measured. Fig. 3 shows one of the examples of PMD generation and measurement, where 100 randomly oriented birefringent sections with ∼0.2-ps DGD each are used to simulate a fiber with ∼2-ps mean DGD. For extraction of the PMD vector using the MMM, we select a sequence of measured SOPs with a spectral step of 71.4 GHz (three times the resolution), which is close to the bandwidth of the PSP [1]. Since PMD can be described by a 3×1 vector, Fig. 3 shows the measured and target DGD and all the three PMD components. The rms error of the estimated DGD is 0.25 ps, ∼10.9% the target mean DGD.

Fig. 4 shows another example of PMD generation, where 100 randomly oriented birefringent sections with ∼0.5-ps DGD each are used to simulate a fiber with ∼5-ps mean DGD. The measured SOPs with 23.8-GHz spectral step are used for MMM. For both Figs. 3 and 4, the variance of PMD with frequency indicates all-order PMD effects. The rms error of the estimated DGD is 0.78 ps, ∼14.6% the target mean DGD.

We carried out the all-order PMD generation experiments 40 times with mean DGDs ranging from 2 to 5 ps. The average ratios of the rms errors and the target mean DGDs in the 5-ps mean DGD case (20 experiments) and 2-ps mean DGD case (ten experiments) are ∼16.2% and 12.3%, respectively.

To emulate the statistics of PMD, one can simulate and store the PMD statistics via computer and then apply the stored Jones matrices with a ∼500-ms updating time. Also, one can apply

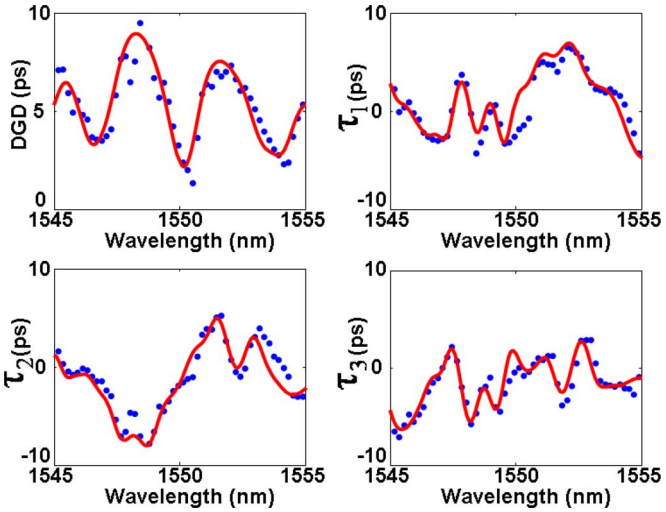

Fig. 4. Measured (dots) and target (solid lines) profiles of DGD and three PMD components for 5-ps mean DGD.

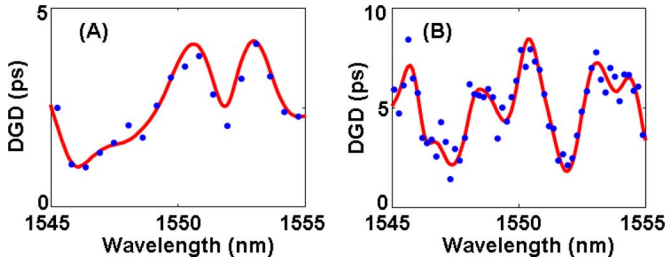

Fig. 5. Simulations comparing estimated DGD curves (dots) with both SOP measurement errors and LCM calibration errors to target DGD curves (solid lines). The mean DGDs in (A) and (B) are ∼2 and ∼5 ps, respectively.

importance sampling techniques [9] to emulate PMD effects involving low probability events of large DGD, which helps us to study PMD more efficiently.

IV. Error Analysis

Theoretically, the PMD generator can accurately generate mean DGD up to ∼10 ps with the resolution of 11.6 GHz. However, the PMD measurement system is limited by the resolution of the polarimeter (23.2 GHz) and can only accurately measure up to ∼5-ps mean DGD. Here the generation/measurement limits are taken as 1/8 of the inverse resolution [1]. The errors of the estimated PMD compared to the target PMD are mainly due to two issues: 1) SOP measurement errors induced by the finite spectral resolution of the polarimeter; 2) LCM calibration errors. By examining the angles on the Poincare sphere between the measured output SOPs corresponding to 0° linear and RHC input SOPs, we estimate the standard deviation (S.D.) of the SOP measurement errors is ∼5° for the 5-ps mean DGD case, and ∼2.5° for two 2-ps mean DGD case. The S.D. of the LCM calibration errors is ∼3°. We have performed simulations taking into account these errors in PMD generation and measurement. One hundred randomly oriented birefringent sections with ∼0.5-ps DGD each are used to simulate a fiber with ∼5-ps mean DGD. We calculate the exact phases for each LCM layer corresponding to the simulated Jones matrix and then add random Gaussian noise with 0 mean and 3° S.D. With the resulting Jones matrix, we calculate the output SOPs corresponding to 0° linear and RHC input SOPs. After that, measurement error is taken into account by adding Gaussian noises with 0 mean and 5° S.D. to the output SOPs. PMD vectors are then calculated based on the output SOPs including measurement error using MMM. The simulation covers 10-nm bandwidth and the sampling spacing for PMD generation and measurement are 11.6 and 23.2 GHz, respectively. We carried out the simulation independently 1000 times. The average ratio of the rms errors of the estimated DGDs and the target mean DGDs is 15.8%. We did the same simulation for the 2-ps mean DGD case (2.5° S.D. of SOP measurement errors), with 11.6-GHz resolution for PMD generation and 69.6-GHz resolution for PMD measurement. The average ratio of the rms errors of the estimated DGDs and the target mean DGDs is 10.6% (over 1000 simulations). The simulation accounts well for the errors in PMD generation measured in the experiments. Fig. 5 shows an example of the simulation results for both the 2- and 5-ps mean DGD cases.

V. Conclusion

We have demonstrated a pulse-shaper-based deterministic PMD generator with the capability of generating arbitrary desired frequency-dependent PMD profiles with mean DGDs ranging from 2 to 5 ps over a 10-nm bandwidth.

Acknowledgment

The authors acknowledge S. X. Wang, L. Xu, and D. E. Leaird for their contributions.

References

[1] H. Kogelnik, R. M. Jopson, and L. E. Nelson, , I. P. Kaminow and T. Li, Eds., "Polarization mode dispersion," in *Optical Fiber Telecommunications IVB-Systems and Impairments*. New York: Academic, 2002, p. 723.

[2] L.-S. Yan, S. X. Yao, M. C. Hauer, and A. E. Willner, "Practical solutions to polarization-mode-dispersion emulation and compensation," *J. Lightw. Technol.*, vol. 24, no. 11, pp. 3992–4005, Nov. 2006.

[3] S. X. Wang and A. M. Weiner, "Fourier pulse-shaper-based high-order differential group delay emulator," *Opt. Express*, vol. 15, pp. 2127–2138, Mar. 2007.

[4] A. M. Weiner, "Femtosecond pulse shaping using spatial light modulators," *Rev. Sci. Instrum.*, vol. 71, pp. 1929–1960, May 2000.

[5] J. P. Gordon and H. Kogelnik, "PMD fundamentals: Polarization mode dispersion in optical fibers," in *Proc. Nat. Acad. Sci.*, Apr. 2000, vol. 97, pp. 4541–4550.

[6] S. X. Wang and A. M. Weiner, "A complete spectral polarimeter design for lightwave communication systems," *J. Lightw. Technol.*, vol. 24, no. 11, pp. 3982–3991, Nov. 2006.

[7] R. M. Jopson, L. E. Nelson, and H. Kogelnik, "Measurement of second-order polarization-mode dispersion vectors in optical fibers," *IEEE Photon. Technol. Lett.*, vol. 11, no. 9, pp. 1153–1155, Sep. 1999.

[8] G. J. Foschini and C. D. Poole, "Statistical theory of polarization dispersion in single mode fibers," *J. Lightw. Technol.*, vol. 9, no. 11, pp. 1439–1456, Nov. 1991.

[9] G. Biondini and W. L. Kath, "Polarization-mode dispersion emulation with maxwellian lengths and importance sampling," *IEEE Photon. Technol. Lett.*, vol. 16, no. 3, pp. 789–791, Mar. 2004.